Palaeogeography, Palaeoclimatology, Palaeoecology 471 (2017) 82–95

Contents lists available at ScienceDirect

Palaeogeography, Palaeoclimatology, Palaeoecology

journal homepage: www.elsevier.com/locate/palaeo

Comparison of deeply buried paleoregolith profiles, Norwegian North Sea, with outcrops from southern Sweden and Georgia, USA — Implications for petroleum exploration

Lars Riber [a,*], Henning Dypvik [a], Ronald Sørlie [b], Syed Asmar Aal-E-Muhammad Naqvi [a], Kristian Stangvik [a], Nikolas Oberhardt [a], Paul A. Schroeder [c]

[a] Department of Geosciences, University of Oslo, P.O. Box 1047, Blindern, NO-0316 Oslo, Norway
[b] Lundin Norway AS, Strandveien 4, NO-1366 Lysaker, Norway
[c] Department of Geology, University of Georgia, 210 Field St., Athens, GA 30602-2501, USA

ARTICLE INFO

Article history:
Received 8 February 2016
Received in revised form 24 January 2017
Accepted 31 January 2017
Available online 3 February 2017

Keywords:
Paleoregolith
Mesozoic weathering
Utsira High
North Sea
Petroleum reservoir
Surface paleoregolith

ABSTRACT

For the first time on the Norwegian Continental Shelf, deeply buried paleoregolith profiles have been identified as part of the petroleum reservoirs in recently discovered oil fields on the Utsira High, Norwegian North Sea. Reservoir properties (porosity and permeability) in the granitic basement on the Utsira High are mainly the result of physical and chemical alteration of the rock occurring in the near-surface environment during sub-aerial exposure of the high in the Mesozoic. Evaluating the reservoir potential of altered basement rocks requires a different approach than in conventional petroleum exploration. In this paper, macroscopic, mineralogical and micromorphological alteration features observed in two deeply buried paleoregolith profiles are compared with surface paleoregoliths from Ivö Klack, Sweden and Georgia, USA. The paleoregolith profiles are subdivided into specific weathering facies (altered coherent rock facies, saprock facies and saprolite facies) based on the rock fabric and mechanical strength. The reservoir potential of each weathering facies is controlled by the type and degree of alteration. In the altered coherent rock facies, porosity and permeability is mainly controlled by joints and microfractures that developed prior to subaerial exposure of the granitic pluton. In the saprock facies, intensified chemical dissolution of plagioclase enhanced porosity and the development of mesofractures improved the connectivity between pores. In the saprolite facies, progressive dissolution of plagioclase creates porosity, but the precipitation of clays within voids and mesofractures has a destructive effect on the overall reservoir properties. The deeply buried paleoregolith profiles from the Utsira High display comparable macroscopic, mineralogical and micromorphological alteration features to what was observed in surface paleoregoliths from Ivö Klack and Georgia. Outcrop studies may therefore be an important tool when evaluating the reservoir potential in subsurface paleoregoliths.

1. Introduction

On the Utsira High, Norwegian North Sea (Fig. 1A) hydrocarbon reservoirs were recently discovered in deeply buried paleoregolith profiles (Riber et al., 2015; Sørlie et al., 2014, 2016). The discovery represents the first time altered and fractured basement rocks are identified as petroleum reservoirs on the Norwegian Continental Shelf. The present paper extends two previous studies from the area (Riber et al., 2015, 2016). By comparing deeply buried paleoregoliths from the Utsira High with outcrops from Georgia, USA (Fig. 2A) and Ivö Klack, Sweden (Fig. 2B), this study will attempt to evaluate how physiochemical alteration in the Critical Zone affected the reservoir quality in the granitic basement rocks on the Utsira High.

Studies of outcrops are common and often needed when constructing subsurface models of conventional siliciclastic and bioclastic petroleum reservoirs (Grammer et al., 2004) as drill cores are normally far between and only provide limited three-dimensional resolution. Suitable outcrops for comparison were identified from Georgia, USA (Fig. 2A), Ivö Klack, Sweden (Fig. 2B), and Bornholm, Denmark (Fig. 2B). The present paper will compare the results from the Utsira High with the results from Georgia and Ivö Klack, while comparable results from Bornholm, Denmark are presented in an accompanying paper (Tan et al., 2017). Recent H-O isotope studies from kaolins in the Cenozoic weathering sections from Georgia, USA and the Mesozoic weathering sections from Ivö Klack and Bornholm, suggests subaerial formation under humid and subtropical conditions (Gilg et al., 2013), that may

* Corresponding author.
E-mail address: lars.riber@geo.uio.no (L. Riber).

http://dx.doi.org/10.1016/j.palaeo.2017.01.043
0031-0182/

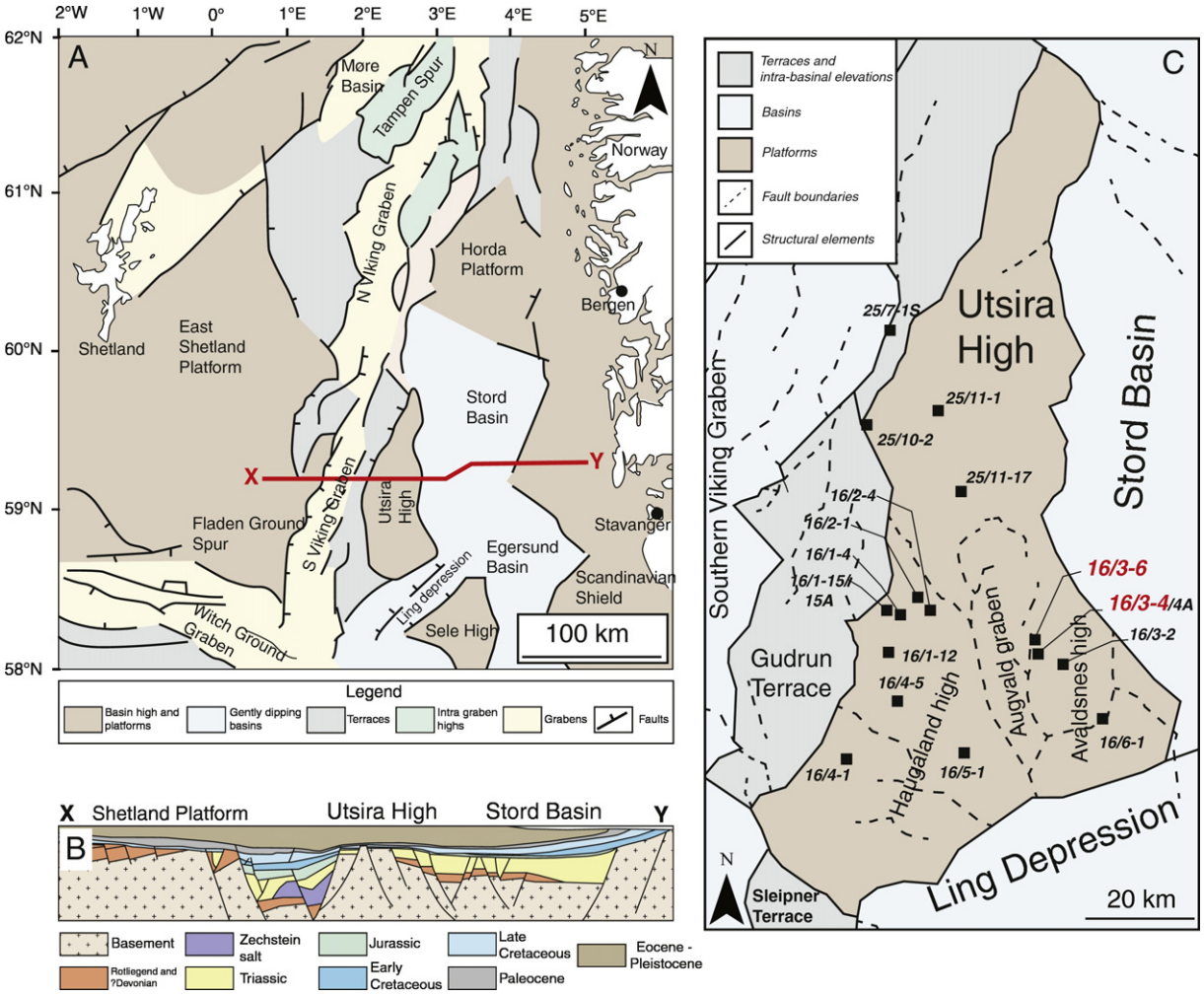

Fig. 1. A) Regional map of the North Sea area (modified from Gregersen et al., 1997) with cross-section marked X-Y. B) Cross-section (X-Y) of the South Viking Graben (modified from Ziegler, 1992). C) Map showing major structural elements on the Utsira High and location of eighteen wells penetrating basement rocks. The two wells included in this study (16/3-4 and 16/3-6) in red.

have been comparable to Mesozoic northern North Sea climatic conditions (Lidmar-Bergström, 1982; Hallam et al., 1993; Abbink et al., 2001; Vajda and Wigforss-Lange, 2009; Nystuen et al., 2014).

In the first comprehensive study of altered basement rocks on the Norwegian Continental shelf, Riber et al. (2015) found that reservoir quality in crystalline rocks from 18 different wells on the Utsira High (Fig. 1C) varied greatly as a function of type and degree of alteration. Based on detailed clay mineralogical, petrographical and geochemical studies Riber et al. (2016) discussed alteration features resulting from near-surface processes in two-well developed paleoregolith profiles (wells 16/1-15 and 16/3-4) (Fig. 1C). The minimal postweathering alteration (diagenetic reactions) observed in the paleoregolith profile in well 16/3-4 (Riber et al., 2016) makes the paleoregolith profile from this well suitable for comparison with a deeply buried paleoregolith profile in well 16/3-6 (Fig. 1C) located about 1 km north of 16/3-4, and surface paleoregolith profiles from Georgia, USA (Fig. 2A) and Ivö Klack, southern Sweden (Fig. 2B).

The coupled near-surface interactions of biochemical and physical processes in the Critical Zone are responsible for the alteration of solid rock to regolith (weathering profile) and soil (Brantley et al., 2006, 2007; Buss et al., 2008; Lin, 2010). Generally a regolith may be divided into three weathering facies based on the degree of recognizable primary rock structures and the mechanical rock strength: the altered coherent rock facies, saprock facies, and saprolite facies (Velde and Meunier, 2008). When considering the regolith as a medium through which fluids can migrate and be stored, the recognition of weathering facies is of great importance as each facies displays contrasting hydraulic properties (porosity and permeability) (O'Brien and Buol, 1984; Acworth, 1987; Schoeneberger and Amoozegar, 1990; Wright and Burgess, 1992; Driese et al., 2001; Négrel, 2006; Velde and Meunier, 2008; Pagliai and Kutilek, 2008; Zauyah et al., 2010). The porosity and permeability in the weathered rock are mostly controlled by fractures and voids. Fractures are particularly important as pathways for the ingress of formation waters and the voids are created from the dissolution of labile minerals and become more important with progressive chemical attack (Acworth, 1987; Wright, 1992; Nelson, 2001; Velde and Meunier, 2008; Zauyah et al., 2010; Jin et al., 2011; Borrelli et al., 2012; Bazilevskaya et al., 2013). With advanced chemical weathering, the neoformation of phyllosilicates and hydroxides will clog previously formed voids and fractures and hence have a negative impact on reservoir quality (Acworth, 1987; Driese et al., 2001; Meunier, 2005; Pagliai and Kutilek, 2008; Zauyah et al., 2010).

Most soils and regoliths are the products of multiple environments ranging over pedogenic time and may therefore be viewed as polygenetic (Molina et al., 1991; Richter and Yaalon, 2012). Furthermore, paleoregoliths are defined as weathering formations that were produced in a geomorphologic and/or climatic environment different from the present one (Battiau-Queney, 1996). In this context both the deeply buried weathering profiles from the Utsira High, and surface weathering sections from Georgia (Schroeder et al., 1997; Schroeder

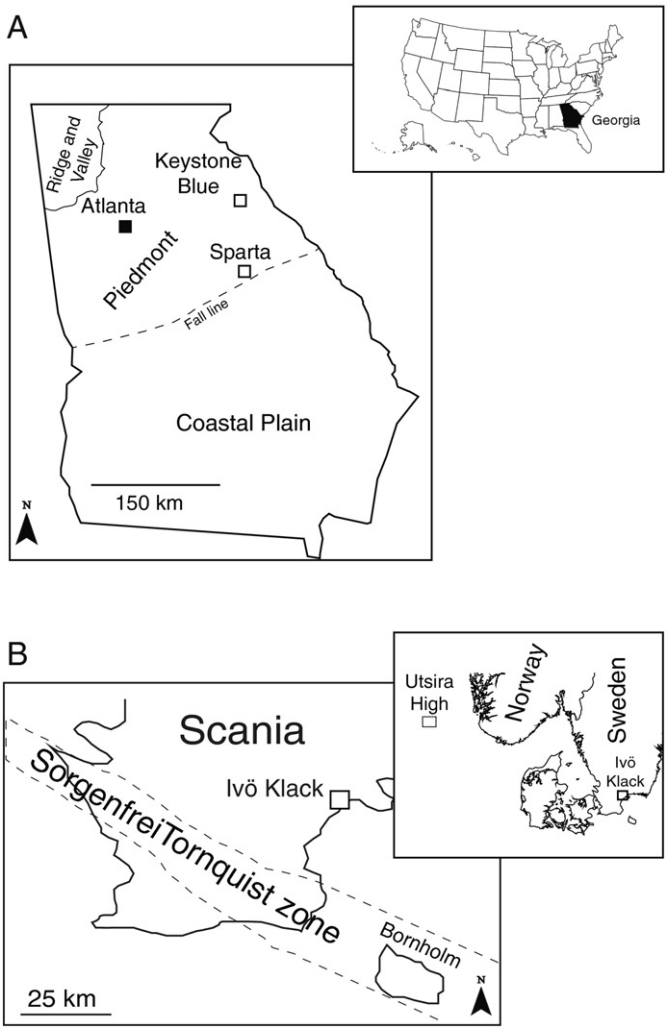

Fig. 2. Locations of surface paleoregolith profiles. A) Map of Georgia, USA. The Keystone Blue quarry and the Sparta quarry are marked by open squares. The Fall Line marks the boundary between the Coastal Plain and the Piedmont. B) Map of southern Sweden (Scania) showing the location of Ivö Klack and Bornholm in relation to the Sorgenfrei Tornquist Zone.

and West, 2005) and Ivö Klack (Lidmar-Bergström, 1982, 1993, 1995, 1999; Lidmar-Bergström et al., 1997) may be regarded as polygenetic paleoregoliths and paleosols.

Recognition of deeply buried paleoregoliths is complicated by the possibility of postweathering diagenetic or hydrothermal alteration (Nesbitt and Young, 1989; Rainbird et al., 1990; Ziegler and Longstaffe, 2000; Retallack, 2001; Driese et al., 2007; Srivastava and Sauer, 2014; Liivamägi et al., 2015). Rock materials associated with basement unconformities are particularly vulnerable to additional alteration, produced by increased permeability and reactivity of the weathered material relative to the fresh rock (Sutton and Maynard, 1992, 1993; Sutton and Maynard, 1996). Furthermore, diagnostic identification of paleoweathering profiles ideally requires the identification of pedogenic features, but paleoregoliths have low potential of preservation and the overlying soil horizons are commonly absent (Migoń, 1997; Bahlburg and Dobrzinski, 2011). Regolith profiles developed in the uplands are often eroded and reworked, and only the profiles developed in the lowlands will normally be preserved in the stratigraphic record (Lidmar-Bergström, 1995; Thiry et al., 1999; Sheldon and Tabor, 2009).

The present study compares macroscopic (rock fabric and mechanical strength), mineralogical (whole rock and clay), and micromorphological alteration features observed in deeply buried paleoregoliths from the Utsira High with surface paleoregolith profiles from Ivö Klack, Sweden and Georgia, USA. The aim of this paper is to show the applicability of outcrops when evaluating how reservoir properties were formed and destroyed in the Critical Zone in the deeply buried paleoregolith profiles from the Utsira High. The present study will test if the same mineralogical and petrographical criteria may be used to distinguish specific weathering facies in both deeply buried and surface paleoregolith profiles, and relate the weathering facies to reservoir properties (porosity and permeability). If successful, this method may increase the predictability of finding areas with better reservoir potential in future drilling campaigns.

2. Geological background

The Utsira High, a Silurian–Ordovician batholith (Slagstad et al., 2011; Lundmark et al., 2013) is currently located at about 2 km depth (Ziegler, 1992) (Fig. 1B) but the granitic basement is believed to have been close to the surface from pre Permian times until transgression was completed in early Cretaceous (Vail et al., 1977; Steel and Ryseth, 1990; Ziegler, 1992; Lervik, 2006; McKie and Williams, 2009; Sørlie et al., 2014; Ksienzyk et al., 2013, 2016). Subaerial exposure and weathering of the granitic basement of the Utsira High in the Permian is indicated by the presence of weathered granitic clasts in Permo-Triassic alluvial fan deposits in half grabens on the Haugaland high (Fig. 1C) (Selvikvåg, 2012; Asbjørnsen, 2015; Sørlie et al., 2016). Recent K-Ar dating of illitic clays from paleoregolith material from the area suggests a late Triassic age of formation (Fredin et al., 2014; Fredin pers. comm. 2015). Uncertainties whether the K-Ar ages represent the final weathering episode exist, however, as Riber et al. (2016) could not ascertain the origin of illitic clays in the paleoregolith profiles.

Continuation of subaerial exposure during the Jurassic was promoted by thermal doming of the central North Sea region prior to Upper Jurassic rifting (Vail et al., 1977; Ziegler, 1992) constantly introducing fresh rock material to the "weathering factory" (Brantley et al., 2007). The presence of granitic rock clasts and diverse Nd-isotope signatures in sub-lithic to lithic Jurassic arenites from the Avaldsnes high (Fig. 1C) (Sørlie et al., 2014) indicate a constant influx of material from nearby sources. Similarly, granitic clasts with weathering rinds were observed in immature shallow marine sandstones of Upper Jurassic age, resting on the altered basement in wells on the Avaldsnes high, including the two wells presented in this study (Riber et al., 2015), and in nearby catchments (Sørlie et al., 2014). Deep weathering on the Utsira High during the Mesozoic was likely the western continuation of the time-equivalent paleosurface and associated regoliths onshore Norway (Roaldset et al., 1982; Roaldset et al., 1993; Olesen et al., 2006; Olesen et al., 2013) and southern Sweden and Denmark (Lidmar-Bergström, 1982, 1993, 1995; Lidmar-Bergström et al., 1997; Ahlberg et al., 2003). Cessation of subaerial exposure of the Utsira High coincided with the end of the rifting episode by early Cretaceous followed by passive thermal subsidence (Ziegler, 1992; Nøttvedt et al., 2008) and was associated with the deposition of shallow marine sediments from Upper Jurassic–early Cretaceous across the high (Riber et al., 2015).

3. Field work and analytical methods

Geological analyses and sampling of wells 16/3-4 and 16/3-6 from the Utsira High (Fig. 3) were carried out during several visits at the premises of Weatherford Laboratories, Sandnes from 2012 to 2016. Two complete weathering profiles and overlying soil horizons from northeastern Georgia, USA (Figs. 4A–B), were sampled and studied during field work in the winter 2014 and parts of the results were presented in Stangvik (2015). The profile from Ivö Klack, Sweden (Fig. 4C) was studied during field work in the fall of 2011 and 2012 and the results are partly presented in Naqvi (2013) and Oberhardt (2013).

From all localities the mechanical properties of the rock were noted according to a modified version of the classification proposed by the International Society for Rock Mechanics Commission on

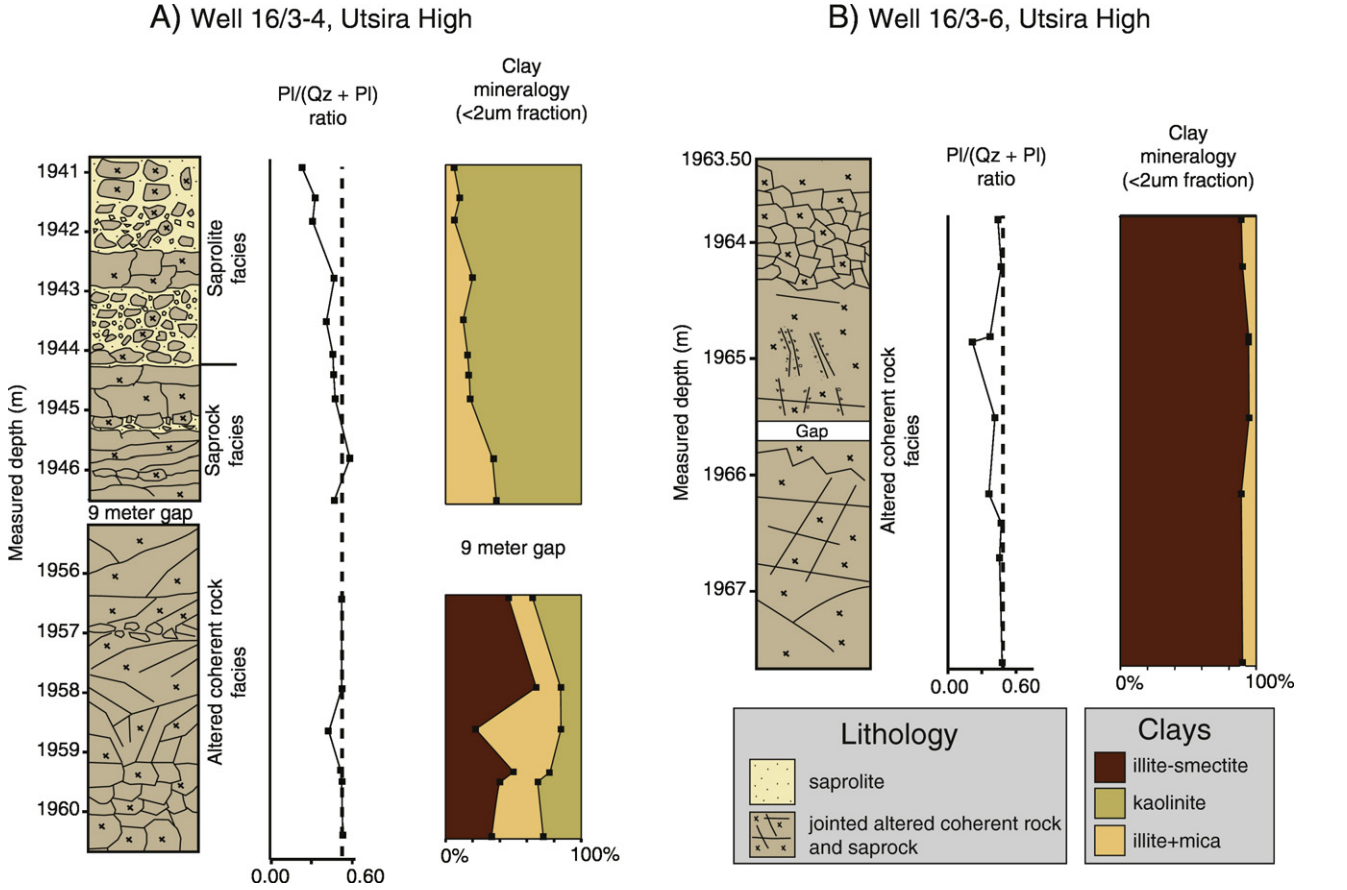

Fig. 3. Sketch logs, Pl/(Qz + Pl) ratios, and clay mineralogy from two deeply buried paleoregolith profiles from the Utsira High. Dotted line represents Pl/(Pl + Qz) ratio in protolith. A) Well 16/3-4. B) Well 16/3-6. Abbreviations: Pl = plagioclase, Qz = quartz.

Standardization of Laboratory and Field Tests (ISRM) (1978). The classification uses a scale from W1–W5, where W1 (fresh): no visible signs of material alteration, W2 (slightly altered): discoloration of discontinuity surfaces, W3 (moderately altered): less than half of the rock material is decomposed, W4 (highly altered): more than half of the rock material is decomposed and, W5 (completely altered): all rock is decomposed, but original rock structure is still largely intact.

The classification scale from W1–W5 forms the basis for subdividing regolith profiles into three weathering facies: in the *altered coherent rock facies*, the original structures are perfectly maintained and only minor alteration of primary minerals has occurred. The *saprock facies* still displays the original rock structure but the mechanical strength of the rock has been reduced due to dissolution of primary minerals. The most altered part of the regolith, the *saprolite facies*, is a friable rock that still retains rock fabric but contains abundant altered primary and secondary minerals. The saprolite gradually loses its original lithic fabric to form soil material towards the surface (Velde and Meunier, 2008; Zauyah et al., 2010).

Whole rock and clay mineralogical studies of the five paleoregolith profiles are based on XRD analyses. XRD analyses were carried out in the Department of Geosciences, University of Oslo on a Bruker D8 ADVANCE (40 kV and 40 m A) diffractometer with Lynxeye 1-dimensional position sensitive detector (PSD), using CuKα radiation. Micronized powder specimens were prepared as randomly oriented bulk samples by the front-loading procedure (Moore and Reynolds, 1997) and analyzed by counting for 0.3 s at steps of 0.01° 2θ from 2 to 65° 2θ. The Rietveld method, using the entire peak profile (Rietveld, 1969), is applied for quantification of mineral abundances using Siroquant V4 (by Sietronics) (Taylor, 1991). The quantification setup follows the five stage procedure suggested by Hillier (2000), with an additional sixth stage based on six cycles of orientation with a damping factor of 0.2.

The clay (<2 μm) fraction was extracted from the whole rock by gravity settling (Moore and Reynolds, 1997). Oriented aggregate mounts were prepared using the Millipore filter transfer method (Moore and Reynolds, 1997) and analyzed after four treatments: air-dried, treated with ethylene glycol (EG) vapor for 24 h, heated at 350 °C for 1 h, and heated at 550 °C for 1 h. XRD data from the <2 μm fraction were recorded by counting for 0.3 s at steps of 0.01°2θ from 2 to 35°2θ. In addition, handpicked biotite grains were crushed and analyzed by XRD separately. Further clay analyses were undertaken with NewMod II, a program designed for simulating one-dimensional oriented aggregate XRD patterns of interstratified clay minerals (Reynolds and Reynolds, 2012).

Standard clay mineral identification of randomly interstratified illite-smectite (R0 I-S), fine-grained mica and illite (I + M), kaolinite, chlorite, vermiculite and hydrobiotite was carried out according to procedures proposed by Moore and Reynolds (1997).

Near-surface chemical alteration trends can be presented in ternary diagrams displaying quartz (resistant to chemical alteration), K-feldspar (semi-resistant to chemical alteration), plagioclase (susceptible to chemical alteration) (Goldich, 1938; Krauskopf and Bird, 1995; Berner and Berner, 2012). On the Qz (quartz)–Pl (plagioclase)–Kfs (K-feldspar) diagram, initial alteration trends will follow the line subparallel to the Pl-Qz line as long as plagioclase dissolution is dominant, and then approach the Qz apex when K-feldspar dissolution commences. The plagioclase (Pl)/(quartz (Qz) + plagioclase (Pl)) ratio represents the abundance of a resistant mineral (Qz) to that more susceptible to alteration (Pl) and was used as a general indicator of weathering.

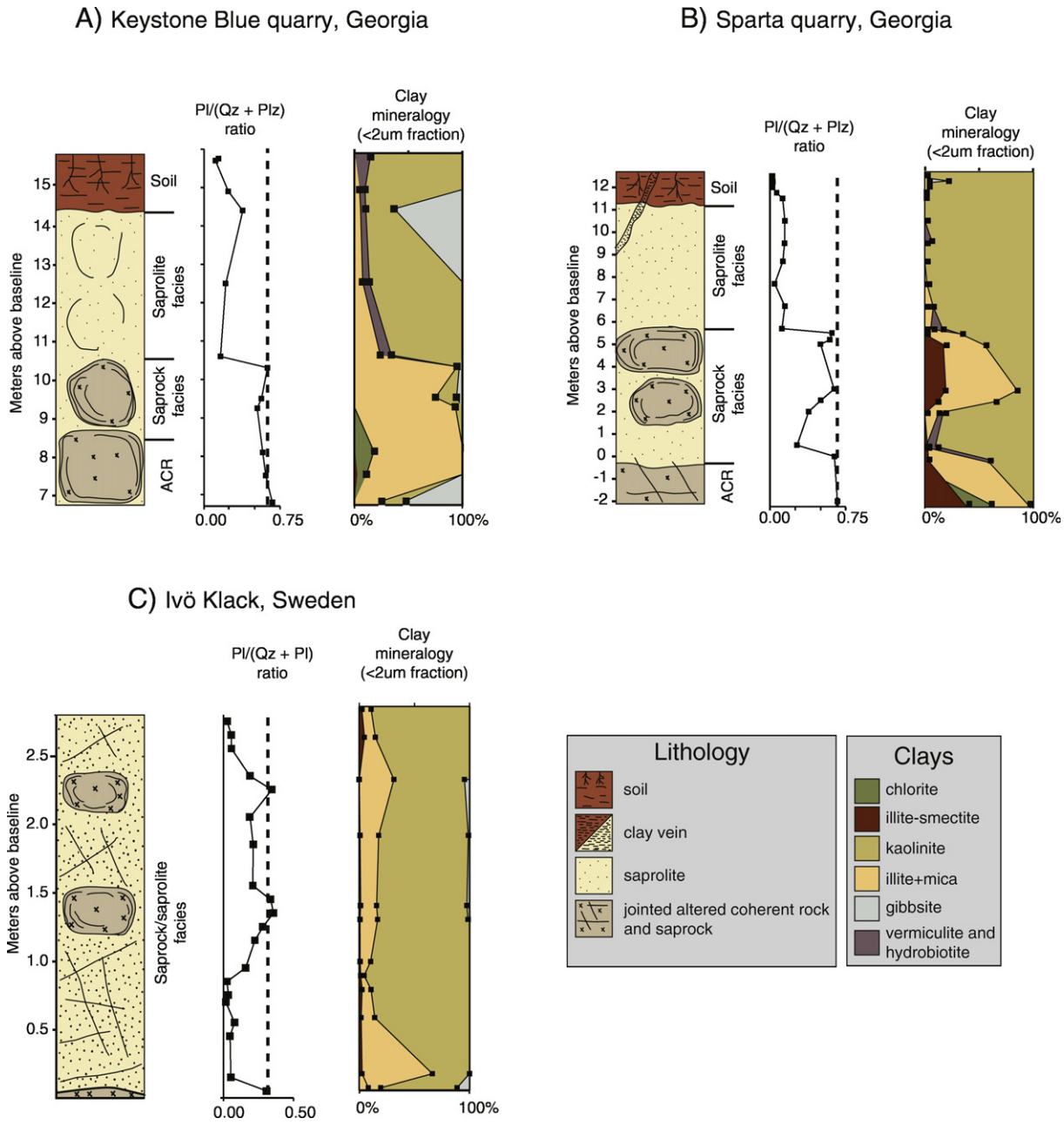

Fig. 4. Sketch logs, Pl(Qz + Pl) ratios, and clay mineralogy from surface paleoregolith profiles. Dotted line represents Pl/(Pl + Qz) ratio in protolith. A) Keystone Blue quarry. B) Sparta quarry. C) Ivö Klack. Abbreviations: ACR = altered coherent rock facies, Qz = quartz, Pl = plagioclase.

Micromorphological alteration features were studied on polished thin sections impregnated with blue epoxy with a Nikon Labophot-Pol petrographic microscope and SEM-EDS (JEOL JSM-6460LV, with a LINK INCA Energy 300 (EDS)) with detectors for secondary-electron images (SEI) and backscattered electron images (BSE).

4. Results

4.1. Utsira High, Norwegian North Sea

The Utsira High is an intrabasinal structural high forming the eastern flank of the Southern Viking Graben and bounded to the east by the Stord Basin (Ziegler, 1992) (Fig. 1). The southern part of the high is informally divided into an eastern structural segment, the Avaldsnes high, and a western, Haugaland high, separated by the Augvald graben (Riber et al., 2015) (Fig. 1C). Well 16/3-4 is located about 900 m east of the Augvald graben, and 16/3-6 is located about 1 km further north and about 1300 m inland from the edge of the graben (Fig. 1C). Protolith compositions from the two paleoregolith profiles are presented in Table 1.

In well 16/3-4 the highly jointed interval from the base of the core up to the gap at level 1955 m is classified as W1–W2, and comprises the altered coherent facies (Table 2, Figs. 3A and 5A). In the altered coherent rock facies biotite alteration is characterized by opening of the mica grains along edges, perpendicular to cleavage. Intragranular microporosity is created by incipient dissolution of the calcic cores of zoned plagioclase crystals (Figs. 6A and 7A). The saprock facies represents the interval from 1946.5 to 1944.25 m (Fig. 3A), as the rock displays decay of mechanical strength (W3–W4) and rounded fracture planes (Table 2, Fig. 5B), increased dissolution of plagioclase (Figs. 6C and 7C), pseudomorphic kaolinitization of biotite (Fig. 6C) and development of partly open mesofractures (Figs. 6C and 7C). The transition to

Table 1
Location of study areas and protolith composition.

Location	Coordinates	Protolith	Rock type	Primary minerals	Mica associaton	Accessory minerals	Reference(s)
16/3-4 (North Sea)	58° 48′ 11.36″ N 02° 43′ 8.3″ E	16/3-4	Medium-grained monzogranite/ granodiorite	Pl > Qz > Kfs	Bt > Ms. > Chl	Ser, Spn, Ap, Rt, Py	Riber et al., 2015
16/3-6 (North Sea)	58° 49′ 7.86″ N 02° 42′ 11.4″ E	16/3-6	Medium-grained granodiorite	Pl–Qz ≫ Kfs	Ms > Bt > Chl	Ser, Spn, Ap, Rt, Py	Riber et al., 2015
Keystone Blue quarry (Georgia)	34° 1′ 7.64″ N 82° 58′ 47.88″ W	Elberton granite	Fine–medium grained monzogranite	Pl > Qz > Kfs	Bt > Chl	Ser, Spn, Ilm, Rt, Mag.	Stormer et al., 1980; Stangvik, 2015
Sparta quarry (Georgia)	33° 17′ 27.07″ N 82° 55′ 58.08″ W	Sparta granite	Fine–medium grained monzogranite	Pl > Qz > Kfs	Bt > Chl	Ser, Spn, Rt,	Stangvik, 2015
Ivö Klack (Sweden)	56° 08′ 22.61″ N 14° 24′ 08.24″ E	Vånga granite	Fine–medium grained monzogranite	Kfs > Qz > Pl	Bt > Ms. > Chl	Ser, Fl, Ep, Aln, Tpz, Spn	Åberg et al., 1985; Naqvi, 2013

Abbreviations (Whitney and Evans, 2010): Qz = quartz, Pl = plagioclase, Kfs = K-feldspar, Ms. = muscovite, Bt = biotite, Chl = chlorite, Ser = sericite, Spn = sphene, Ap = apatite, Rt = rutile, Py = pyrite, Ilm = ilmenite, Mag = magnetite, Fl = fluorite, Ep = epidote, Aln = alanite, Tpz = topaz.

the saprolite facies was observed at 1944.25 m (Fig. 3A) where the granite appears friable (W4–W5) (Fig. 5E) and secondary clay minerals are abundant (Table 2, Figs. 6E and 7E). The pervasive chemical dissolution of plagioclase and accompanying kaolinization advances upwards, resulting in the reduction of plagioclase relative to quartz by about 50% in the saprolite compared to the protolith (Riber et al., 2016) (Figs. 3A and 8). The precipitation of kaolinitic clays within dissolution voids and along mesofractures reduces the connectivity between pores (Figs. 6E and 7E). In addition, Riber et al. (2016) observed brownish clays within mesofractures in the uppermost saprolite samples in 16/3-4 that may represent illuviated pedogenic material from above. The clay mineral assemblage changes from R0 I-S (with about 75–80% expandable layers) and well-ordered, vermicular kaolinite dominating the altered coherent rock facies, to a disordered, platy, and massive kaolinite-dominated saprock and saprolite facies (Riber et al., 2016) (Fig. 3A). Minute pyrite inclusions were observed within splayed biotite grains in the saprolite facies.

The highly jointed paleoregolith profile in well 16/3-6 is classified as altered coherent rock facies (Fig. 3B) because the rock displays only minor reduction of mechanical strength (W1–W2) (Table 2), and the Pl/(Qz + Pl) ratio throughout the paleoregolith interval show only minor variations compared to protolith composition (Fig. 3B). Exceptions are close to open joints, around 1965 m, where the rock appears friable (W4), displays increased Pl/(Qz + Pl) ratios (Fig. 3B) and more pronounced chemical alteration on the Qz–Pl–Kfs diagram (Fig. 8). I-S (with 80–90% expandable layers) dominates the clay fraction throughout the paleoregolith interval, with subordinate kaolinite (1–10%), and traces of I + M and chlorite (Fig. 3B). Microfractures, crossing grain boundaries, were observed in connection with initial intra-granular dissolution of plagioclase (Fig. 7B). Biotite alteration is indicated by splayed wafers observed under the SEM. In addition XRD analysis of handpicked biotite grains shows a reflection around 10.5 Å that did not expand upon ethylene glycolation and was destroyed after the last heat treatment. The reflection around 10.5 Å is interpreted to represent the presence of interstratified biotite-vermiculite. Similar to 16/3-4, pyrite inclusions were also observed within altered biotite in 16/3-6.

4.2. Georgia, USA

In the southeastern United States the Mesozoic and Cenozoic Coastal Plain is delineated along the Fall Line that separates it at the surface from a large plateau region dominated by igneous and metamorphic rocks, known as the Piedmont (Markewich et al., 1990) (Fig. 2A). Two deeply weathered profiles (from fresh rock to the soil) were studied, from the Keystone Blue quarry and the Sparta quarry (Table 1, Fig. 4A–B).

The studied weathering sections from the Keystone Blue and Sparta quarries represent the transition between the altered coherent rock and saprock facies, through the saprolite facies, and grading upwards to the soil horizons (Table 2, Fig. 4A–B). Protolith samples from the Elberton and Sparta granites were collected from exposed fresh granite (W1) deeper down in the quarries and both classify as one-mica (biotite) medium-grained monzogranite (Stangvik, 2015) (Table 1). The granites in both sections are jointed, but are more pronounced in the Sparta profile, forming well-defined rectangular granitic blocks (Fig. 5B).

The altered coherent rock facies (Fig. 4A–B) comprises rocks that are classified from W1–W3 on the weathering scale. In the field, alteration in the altered coherent rock facies is restricted to open joints where oxidation of Fe-rich minerals and incipient hydrolysis are indicated by reddish color. In samples from the altered coherent rock–saprock facies vermicular kaolinite and R0 I-S, with 95% expandable layers were identified in XRD (Fig. 4A–B) and observed under the SEM within intragranular micropores in plagioclase grains. Biotite is commonly relatively unaltered, but incipient alteration is indicated by fan or splay development along edges and by the identification of interstratified biotite-vermiculite in XRD.

The saprock facies was recognized in the field by the appearance of corestones with rounded edges and friable exfoliation shells, separated by a thin zone of saprolitic material (Fig. 5D). The saprock exhibits reduced mechanical strength, up to W4 on the weathering scale, and the development of mesofractures and dissolution voids after altered plagioclase was observed under the optical microscope (Table 2, Figs. 6D and 7D). In the Keystone Blue profile gibbsite is enriched in the clay fraction from the saprolitic material between corestones (Stangvik, 2015) (Fig. 4A). Samples from the rindlet zone and towards the coherent parts of the corestones in the Sparta profile demonstrate a stepwise inward reduction of kaolinite and increase in I-S, suggesting a composition similar to the altered coherent rock (Fig. 4B).

The saprock-saprolite boundary facies could be observed in the field as a decay of mechanical rock strength, where most samples are classified as W5 on the weathering scale (Table 2, Fig. 5D). The boundary is characterized mineralogically by a sudden reduction of plagioclase relative to quartz and concomitant increase in kaolin (Fig. 7E), compared to the saprock facies (Fig. 4A–B). In the saprolite facies from the Keystone Blue profile the outline of original corestones is preserved but the rock material is totally disintegrated, as is the surrounding rock (Fig. 5F). The lower part of the saprolite facies in the Sparta section is characterized by a 1 m thick reddish layer where iron oxides were identified, associated with altered biotite (Stangvik, 2015). Under the SEM, kaolin displays elongated, tubular morphologies similar to halloysite

Table 2
Summary of macroscopic (W1–W5), mineralogical (Pl/(Qz + Pl)) and clay), micromorphological alteration features for each weathering facies identified from all five paleoregolith profiles. In addition the most important factors controlling reservoir properties for each weathering facies are listed.

	Weathering facies	Interval (m)	W1–W5	Pl/(Qz + Pl)	Clay mineralogy	Micromorphology	Reservoir properties
16/3-4	Altered coherent rock facies	1960.60–1952 m	W1–W2	Similar to protolith composition	I-S > I + M > Kln	Incipient dissolution of Pl. and minor alteration of Bt.	Por. and perm. controlled by macrofractures. Intracrystalline micropor.
	Saprock facies	1952–1944.25 m	W3–W4	Slight reduction of Pl.	Kln > I + M	Intensified Pl dissolution and pseudo. kaolinitization of Bt.	Intercrystalline por. and mesofractures after plg. dissolution.
	Saprolite facies	1944.25–1940.80 m	W4–W5	Pl reduced by 50% relative to Qz in protolith	Kln ≫ I + M	Pervasive dissolution of Pl and kaolinitization of Bt. Massive Kln occupies pore space.	Voids after Pl dissolution. Clays reduce perm.
16/3-6	Altered coherent rock facies	1963.50–1967.60 m	W1–W2 (W4 close to fracture)	Similar to protolith composition except close to fractures.	I-S > Kln > I + M	Incipient dissolution of Pl and oxidation of Bt.	Por. and perm. controlled by macrofractures. Intracrystalline micropor.
Keystone Blue	Altered coherent rock facies	7–8.5 m	W1–W3	Similar to protolith composition	I + M>Gbs>Kln>Chl>I-S	Incipient dissolution of Pl. and minor oxidation of Bt to hydrobiotite.	Por. and perm. controlled by macrofractures. Intracrystalline micropor.
	Saprock facies	8.5–10.5	W2 (core stones)–W4	Slight reduction of Pl.	I + M > Kln > Gbs	Intensified Pl dissolution and pseudo. kaolinitization of Bt	Intercrystalline porosity and mesofractures after Pl dissolution.
	Saprolite facies	10.5–14.3 m	W4–W5	Sudden reduction of Pl.	Kln > I + M > Vrm and hydr. Bt > Gbs	Pervasive dissolution of Pl. Pseudom. transformation of Bt to Kln and Gbs.	Voids after Pl dissolution. Clays reduce perm.
	Soil	14.3–15.5 m	–	Close to total disappearance of Pl.	Kln > Gbs > Vrm	Organic matter and pedogenic features. Residual Qz and Kln.	Low por. and perm. due to domination of clays and organic matter
Sparta	Altered coherent rock facies	−2–0 m	W1–W3	Similar to protolith composition	I-S > Chl > I + M > Kln	Incipient dissolution of Pl. and minor oxidation of Bt to hydrobiotite.	Por. and perm. controlled by macrofractures. Intracrystalline microporosity
	Saprock facies	0–5.5 m	W2 (core stones)–W4	Reduction of Pl between corestones	Kln > I + M > I-S	Intensified Pl dissolution and pseudo. kaolinitization of Bt.	Intercrystalline por. and mesofractures after Pl dissolution
	Saprolite facies	5.5–11.2 m	W4–W5	Sudden reduction of Pl and decreasing Kfs.	Kln ≫ I + M > Vrm and hydr. Bt > Gbs	Pervasive dissolution of Pl. Pseudom. transformation of Bt to Kln and Gbs.	Voids after Pl dissolution. Clays reduce perm.
	Soil	11.2–12.5 m	–	Close to total disappearance of Pl.	Kln ≫ I + M > Bt > Gbs	Organic matter and pedogenic features. Residual Qz and Kln.	Low por. and perm. due to domination of clays and organic matter
Ivö Klack	Saprolite/saprock facies	0–2.8 m	W2 (in corestones)–W5 (saprolite)	Close to total dissolution of Pl in most altered areas.	Kln ≫ I + M > I-S > Gbs.	Pervasive dissolution of Pl. Pseudom. transformation of Bt to Kln.	Voids after Pl dissolution. Clays reduce perm.

Abbreviations (Whitney and Evans, 2010): Qz = quartz, Pl = plagioclase, Bt = biotite, Kfs = K-feldspar, Kln = kaolinite, I-S = interstratified illite-smectite, I + M = illite and fine-grained mica, Vrm = vermiculite, hydr. Bt = hydrobiotite, Gbs = gibbsite, por. = porosity, perm. = permeability, pseudom. = pseudomorphic.

(Stangvik, 2015). Biotite is pseudomorphically transformed to kaolinite, in some cases to gibbsite, through stages of hydrobiotite and vermiculite. A difference between the two Georgia profiles is the apparent reduction of K-feldspar in the saprolite facies in the Sparta profile, which was not observed in the Keystone Blue section (Fig. 8).

The original granite structure is lost when moving up into the reddish and mottled soil horizon. In the soil horizons organic matter and pedogenic features, such as peds and clay cutans, were commonly observed under the microscope, and the mineralogy is dominated by residual quartz and kaolinitic clay (Table 2, Fig. 4A–B).

4.3. Ivö Klack (Sweden)

Ivö Klack is located in Scania (southern Sweden), north of the Sorgenfrei Tornquist zone that defines the border between the stable Fennoscandian-Baltic Shield and the metastable Danish-Polish Trough (Liboriussen et al., 1987) (Fig. 2B). On Ivö Klack, deep weathering of crystalline basement rocks occurred in humid subtropical–tropical conditions from late Triassic to late Cretaceous times (Gilg et al., 2013; Naqvi, 2013; Oberhardt, 2013). Deep weathering and kaolinitization of the bedrock occurred before partial erosion and late Cretaceous transgression (Lidmar-Bergström et al., 1997; Surlyk and Sørensen, 2010). The hill of Ivö Klack is dominated by the Vånga Granite, a medium–coarse grained foliated and migmatized granite (Lundegårdh, 1978) (Table 1).

The residual paleoregolith investigated at Ivö Klack is a 2.8 m profile through a jointed corestone from the saprock–saprolite facies (Fig. 4C). Weathering along joints within the corestone resulted in a subset of smaller corestones (W2–W3) separated by saprolitic intervals (W4–W5) (Table 2, Fig. 4C). The central parts of the corestone are classified as altered coherent rock facies (W2), with a gradual decay of mechanical rock strength outwards. The degree of weathering is reflected in the dissolution of sercitized plagioclase demonstrated by the low Pl/(Qz + Pl) ratios (Fig. 4C) and the clustering of samples close to the Qz–Kfs join on the Qz–Pl–Kfs diagram (Fig. 8). The rock composition within joints is nearly depleted in plagioclase, but the plagioclase content gradually increases towards the center of the preserved corestone (Fig. 4C). Perthitic feldspars demonstrate preferential dissolution of

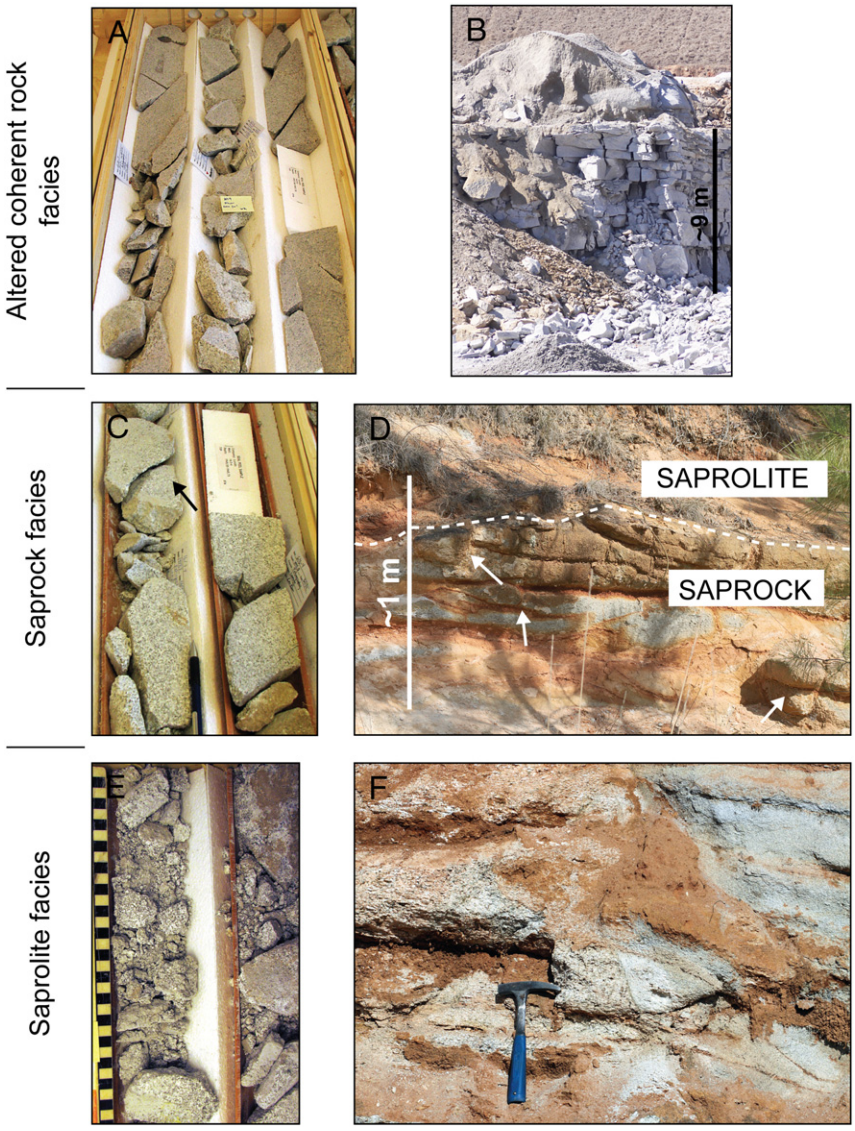

Fig. 5. Comparison of macroscopic alteration features in weathering facies from deeply buried paleoregolith in 16/3-4 with surface paleoregolith profiles in Georgia. Diameter of core is 4 in (10.16 cm). A) Jointed altered coherent rock facies from 16/3-4. B) Severely jointed altered coherent rock facies from the Sparta quarry, Georgia. C) Smoothed joints (arrow) in saprock facies from well 16/3-4. D) Rounded blocks (arrows) in the saprock facies from Keystone Blue quarry. E) Completely disintegrated saprolite from well 16/3-4. F) Completely disintegrated saprolite from Keystone Blue quarry. Size of hammer is 28.5 cm.

albitic exsolution lamellas (Fig. 6F) (Naqvi, 2013). Biotite alteration is characterized by opening of wafers perpendicular to cleavage and pseudomorphic transformation to kaolinite.

The clay mineralogy is dominated by kaolin, between 70 and 96 wt%, with subordinate I + M, R0 I-S, and gibbsite (Table 2, Fig. 4C). Within the most weathered areas the amounts of kaolin reach up to 16 wt% of the total rock, compared to <1 wt% in central parts of corestones (Fig. 4C). Kaolin was observed within dissolution voids in plagioclase, and displays up to 20 μm thick vermicular kaolinite crystals and tubular needles resembling halloysite. Intergranular porosity is mainly created by dissolution of plagioclase, and intragranular porosity from dissolution of exsolution lamellas in K-feldspar (Fig. 6F). In the saprolite facies, voids after feldspar dissolution and mesofractures are commonly occupied by kaolinitic clays (Table 2, Fig. 6).

5. Discussion

The two paleoregolith profiles (wells 16/3-4 and 16/3-6) from the eastern part of the Utsira High (Fig. 1C) and surface paleoregoliths from Ivö Klack, Sweden and Georgia, USA are subdivided into weathering facies that display similar macroscopic (Fig. 5), mineralogical (Figs. 3, 4 and 8) and micromorphological (Figs. 6 and 7) alteration features (Table 2).

The altered coherent facies is recognized in cores and outcrops by the low reduction of mechanical strength (W1–W2). In addition, Pl/(Pl + Qz) ratios display only minor deviance from protolith composition, and clay mineralogy is dominated by R0 I-S and I + M over kaolinite (Table 2). Reservoir properties in the altered coherent rock facies are mainly controlled by joints (Fig. 5B) and microfractures (Dewandel et al., 2006; Stober and Bucher, 2007), likely created by extrinsic stresses related to local tectonism or erosion of overburden, and by intrinsic stresses induced by pore fluid pressures or by thermal cooling and contraction of the pluton (Bergbauer and Martel, 1999; Nelson et al., 2000; Cuong and Warren, 2009; Graham et al., 2010). Unweathered granite generally displays low porosity (<1%) in the rock mass between joints (Graham et al., 2010), but when the granitic pluton reaches the Critical Zone, the joints and microfractures act as pathways for meteoric water and thus commence the conversion of low-porosity rock to regolith

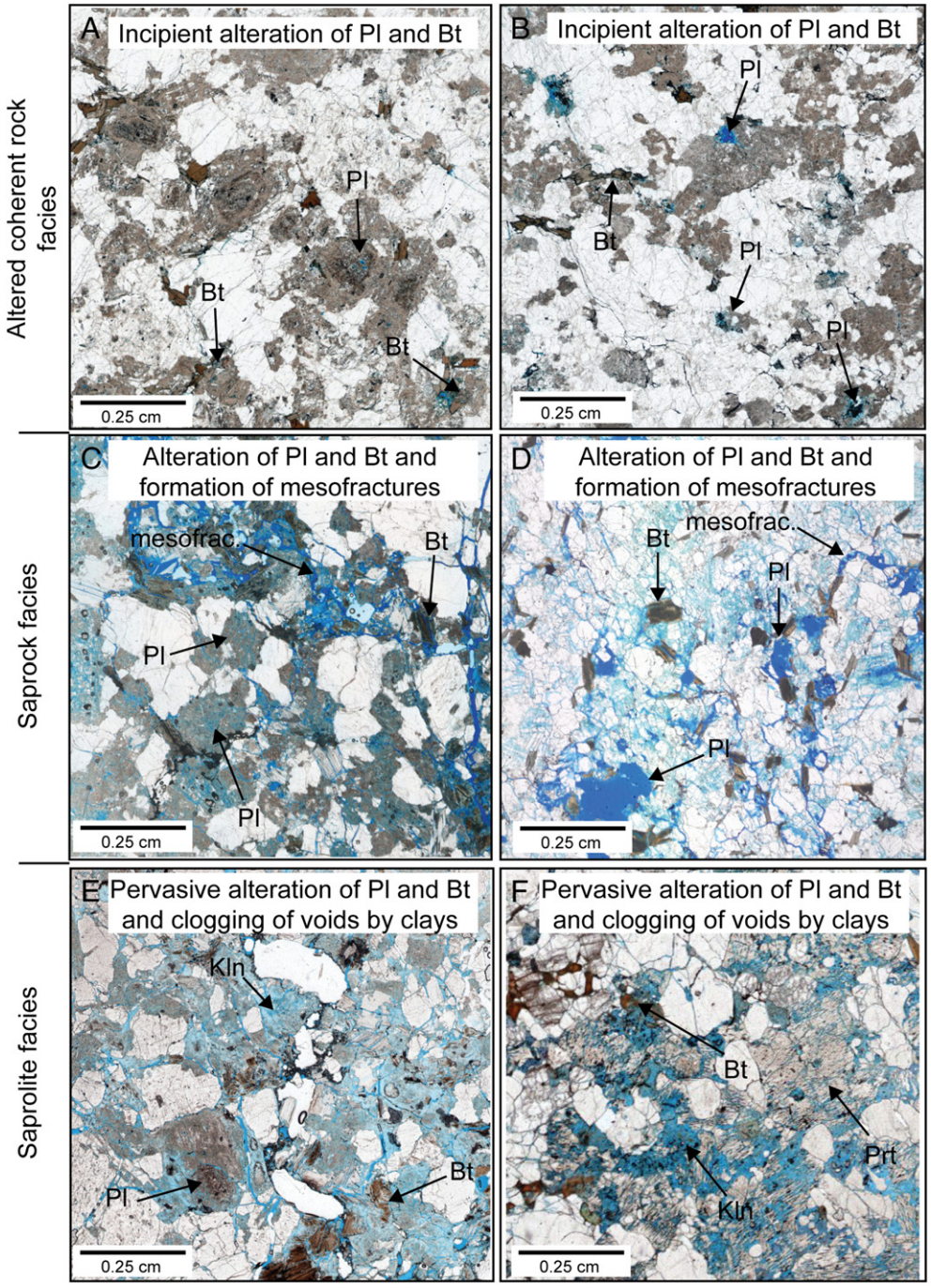

Fig. 6. Thin section images comparing reservoir properties in the three weathering facies from paleoregolith profiles from the Utsira High, Ivö Klack and Keystone Blue. Voids and fractures indicated by blue epoxy. A) Altered coherent rock facies in well 16/3-4. B) Altered coherent rock facies in well 16/3-6. C) Saprock facies in well 16/3-4. D) Saprock facies in Keystone Blue. E) Saprolite facies in well 16/3-4. F) Saprolite facies from Ivö Klack Abbreviations: Pl = plagioclase, Bt = biotite, Kln = kaolinite, mesofrac. = mesofractures.

(Navarre-Sitchler et al., 2015). In the present study, intragranular dissolution of calcic cores of zoned plagioclase crystals was observed as the first formation of porosity (Figs. 6A–B and 7A–B). Incipient oxidation of iron-bearing minerals in the lower parts of the paleoregolith profiles is indicated by the reddish color along exfoliation planes in the surface paleoregoliths in Georgia. Interstratified biotite-vermiculite is an early intermediate phase in the transformation of biotite to kaolinite (Rebertus et al., 1986; Kogure and Murakami, 1996) and was identified at the base of the saprock profile in the Sparta quarry, and in the altered coherent rock facies in 16/3-6. Spheroidal fracturing, induced by biotite expansion after Fe-oxidation (Buss et al., 2008) and vermiculization (Le Pera and Sorriso-Valvo, 2000; Fletcher et al., 2006; Scarciglia et al., 2007; Bazilevskaya et al., 2013; Parizek and Girty, 2014; Webb and Girty, 2016) has been reported to be one of the earliest reactions responsible for porosity developments in crystalline rocks by weathering (Bazilevskaya et al., 2015).

The saprock facies fabric is recognized in the field by rounded boulders separated by thin layers of saprolitic material (Table 2). In cores from well 16/3-4, fracture planes in the saprock facies are rounded and the interval possibly represents a section through corestones (Fig. 5C) similar to what was observed in outcrops. The observed vertical zonation of clay minerals in 16/3-4, from coexisting R0 I-S and kaolinite in

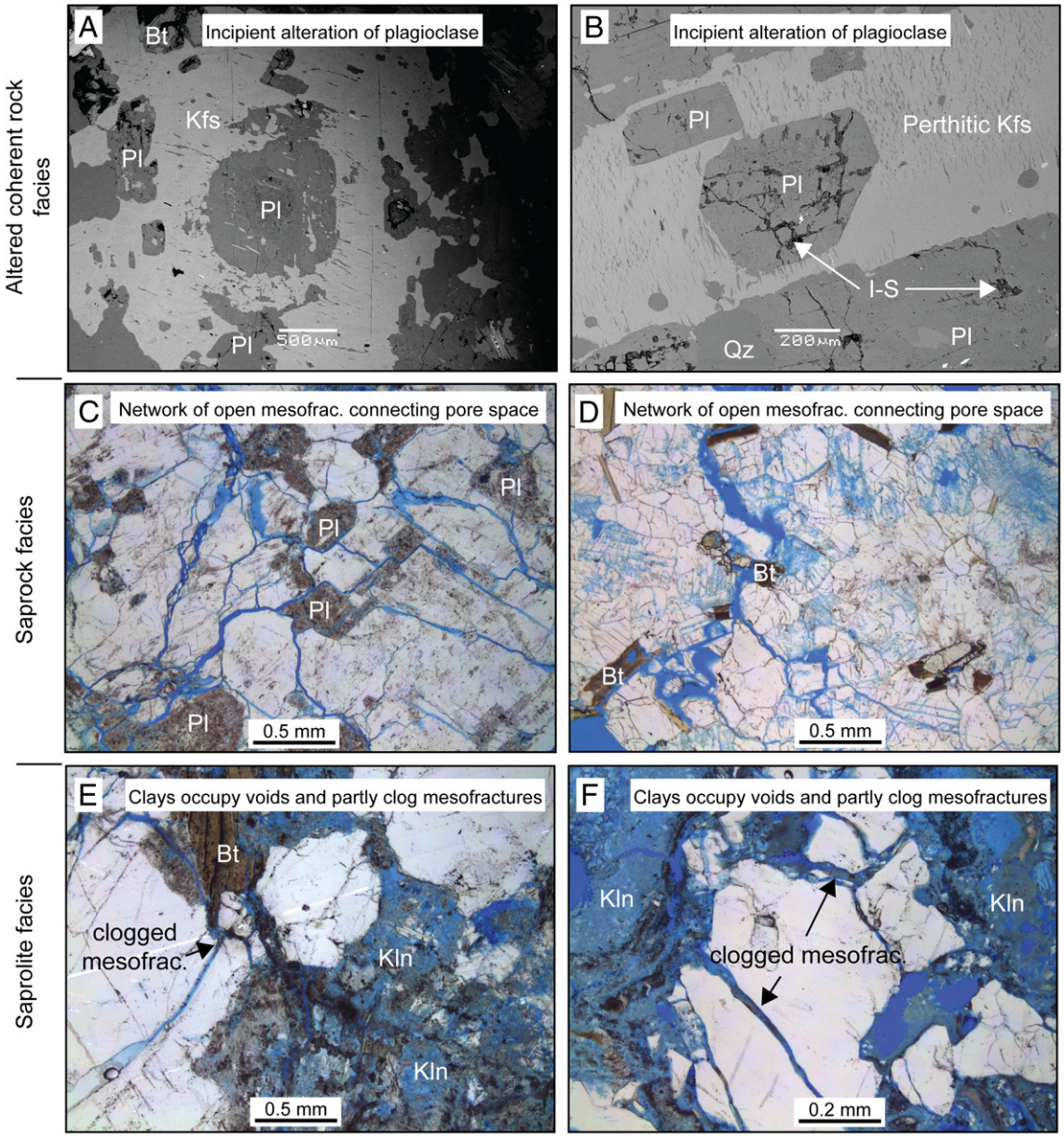

Fig. 7. Backscatter SEM images and micrographs comparing micromorphological features in weathering facies from deeply buried paleoregolith with surface paleoregolith. Voids and fractures indicated by blue epoxy. A) SEM image of mantled feldspar in altered coherent rock facies in well 16/3-4. Note incipient alteration of plagioclase. B) SEM image of mantled perthitic feldspar from altered coherent rock facies in 16/3-6. Note incipient alteration of plagioclase and precipitation of I-S in dissolution voids. C) Micrographs showing increased dissolution of plagioclase in saprock facies in well 16/3-4. Note the presence of open mesofractures. D) Micrograph showing increased dissolution of plagioclase and alteration of bitotite in the saprock facies in profile from the Keystone Blue quarry. Note the presence of open mesofractures. E) Micrograph showing pervasive dissolution of plagioclase and precipitation of kaolinite in voids and mesofractures in saprolite facies from well 16/3-4. F) Micrograph showing pervasive dissolution of plagioclase, alteration of biotite, and precipitation of kaolinitic clays in voids and mesofractures in saprolite facies from the Sparta quarry. Abbreviations: Qz = quartz, Pl = plagioclase, Bt = biotite, Kfs = K-feldspar, Kln = kaolinite, I-S = interstratified illite-smectite, mesofrac. = mesofracture.

the saprock towards increased kaolinization in the saprolite (Fig. 3) is comparable to observations from the Sparta profile (Fig. 4B) and through the corestone section from Ivö Klack (Fig. 4C). Although porosity within residual corestones may be extremely low (Buss et al., 2008), the density of microcracks and intragranular weathering of plagioclase crystals increase towards the rindlet zone of the corestones and towards the saprolite (Buss et al., 2008), and thus enhance reservoir quality.

In the transition from the saprock facies to saprolite facies in 16/3-4 the intensified chemical attack on plagioclase and biotite, and concomitant precipitation of kaolinite are similar to the observations from the studied outcrops (Figs. 6E–F, 7E–F and 8), but the disappearance of plagioclase is more gradual in the deeply buried paleoregolith profile (Fig. 3) than in the surface paleoregolith in Georgia (Schroeder et al., 1997) (Fig. 4A–B). In the saprock and saprolite facies, porosity increases mainly as a result of plagioclase dissolution (Meunier, 2005) (Figs. 6C–F and 7C–F). Mesofractures that developed in the saprock facies contribute to improved connectivity between voids (Figs. 6C–D), but in the saprolite facies increased precipitation of clays within pores and mesofractures likely has a destructive effect on the permeability (Figs. 6E and 7E). Acworth (1987) has reported a similar reduction of permeability in saprolite zones with massive accumulation of clays. Furthermore, in a study of ground-water flow in sedimentary saprolites, Driese et al. (2001) found that the accumulation of illuviated clays in pores and fractures created a low-hydraulic-conductivity barrier. In addition, the decay of

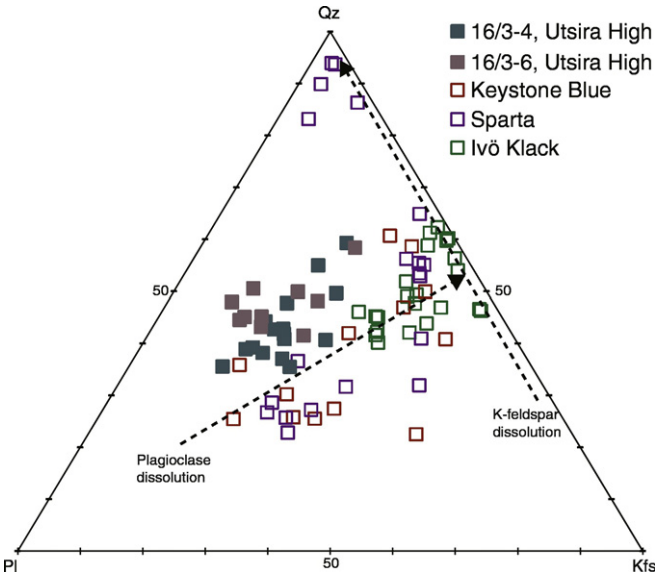

Fig. 8. Ternary diagram showing mineralogical weathering trends from all locations represented by the relative proportions of quartz (Qz), plagioclase (Pl), and K-feldspar (Kfs).

mechanical properties in the saprolite may result in the collapse of the rock structure that causes increased length and tortuosity of fluid pathways (Velde and Meunier, 2008, Pacheco and Van der Weijden, 2012).

Depletion of primary minerals and formation of secondary phases (phyllosilicates and hydroxides) occurs in the Critical Zone through water-rock interactions as a function of time (White and Brantley, 2003). Gibbsite and kaolinite dominate in well-drained systems with high availability of water and strong leaching, whilst illite-smectite is more common in poorly-drained systems with close to stagnant conditions (Velde and Meunier, 2008). In tropical–subtropical regions the regolith profile may display a vertical clay mineralogical zonation. The solution waters are generally neutralized downwards in the profile suggesting a zonation from kaolin clays and gibbsite in the saprolite and saprock facies to 2:1 clay minerals (such as smectite) in altered coherent rock facies (Nahon, 1991; Nesbitt et al., 1997; Eggleton et al., 2008), which is comparable to the results in the present study.

The two deeply buried paleoregolith profiles from the Utsira High experienced partial truncation of the original weathering profile before burial in the Upper Jurassic. In well 16/3-4 the soil horizons were eroded and shallow marine sandstones of Upper Jurassic age (Riber et al., 2015) were deposited on the saprolite facies (Fig. 9). Well 16/3-6 was more deeply truncated and only the altered coherent rock facies is preserved below the Upper Jurassic shallow marine sandstone cover (Fig. 9). The poorer preservation of the paleoregolith observed in 16/3-6 compared to 16/3-4 may have been a result of it being positioned farther inland (Thiry et al., 1999; Sheldon and Tabor, 2009) (Fig. 9), but local variations in the development and preservation of weathering mantles are expected (Meunier, 2005).

During transgression and passive thermal subsidence of the Utsira High from Upper Jurassic, diagenetic alteration of the original weathering mantle most likely took place. The degree of diagenetic chemical alteration in the deeply buried paleoregolith profiles in this study is believed to be minor, but is still uncertain. Riber et al. (2016) identified severe postweathering alteration including precipitation of interstratified serpentine-chlorite in the paleoregolith interval in well 16/1-15 on the western side of the Utsira High (Fig. 1C). The alteration features in well 16/3-4 and 16/3-6 on the Avaldsnes high were, in contrast, interpreted to mainly have been inherited from the subaerial weathering phase and that the reservoir properties of the regolith were created before burial (Riber et al., 2016). The pyrite inclusions observed within altered biotite in both 16/3-4 and 16/3-6, however, are likely the result of interactions with reducing pore fluids during early diagenetic alteration (Wright, 1986; Claeys and Mount, 1991; Riber et al., 2016). Gibbsite was observed in the surface paleoregolith in Georgia and Ivö Klack (Table 2) but not in the deeply buried weathering sections from the Utsira High. Although gibbsite is common in soils, the mineral is less commonly observed in ancient sediments (Curtis and Spears, 1971). If gibbsite was present in the original weathering profile on the Utsira High, the narrow field of stability for gibbsite (Nesbitt and Young, 1989) makes it possible that during burial, increased activity of silica in the pore-space resulted in reaction of gibbsite with soluble silica to form stable kaolinite (Curtis and Spears, 1971; Weaver, 1989; Liivamägi et al., 2015). If any halloysite had been present in the original weathering profiles from the Utsira High, it is likely that the mineral had converted to the more stable phase of kaolinite with ageing or intensified degrees of weathering (Huang, 1974; Tsuzuki and Kawabe, 1983; Dong, 1998; Papoulis et al., 2004; Joussein et al., 2005), or, alternatively, dehydration and possible conversion to kaolinite may have occurred during burial (Huang, 1974) of the Utsira High profiles to about 2 km and bottom hole temperatures of >84 °C (www.npd.no). In addition, mechanical compaction during burial is not discussed in the present paper, but likely had negative impact on reservoir quality (Ramm, 1992; Storvoll et al., 2005) in the deeply buried paleoregolith profiles.

6. Conclusion

The method presented here has successfully been applied to subdivide deeply buried paleoregolith profiles from the Utsira High, Norwegian North Sea, into specific weathering facies by comparing macroscopic, mineralogical and micromorphological alteration features with surface paleoregoliths from Georgia, USA and Ivö Klack, Sweden. The results show that chemical alteration of crystalline rocks in the Critical Zone was responsible for both the formation and the destruction of reservoir properties in the studied sections. The three weathering facies display contrasting type and degree of alteration that exerts control on the overall reservoir quality of the paleoregolith. In the altered coherent rock facies, reservoir properties are mainly related to previously formed joints. Initial porosity developments in the altered coherent rock facies are likely the result of early alteration and expansion of biotite and incipient plagioclase alteration. In the saprock facies, plagioclase dissolution becomes the dominant porosity forming process and the growth of mesofractures enhance the connectivity between dissolution voids. As mineral dissolution intensifies in the saprolite facies, the increased precipitation of kaolinitic clays clogs voids and mesofractures. In addition, the decay of mechanical properties result in the collapse of the rock structure and thus the overall reservoir quality is reduced.

By comparing the deeply buried paleoregolith profile with complete surface weathering sections from Georgia, it is interpreted that deep erosion of the original regolith and soil horizons on the Utsira High occurred before and during transgression in Upper Jurassic (Fig. 9A–B). In well 16/3-4 all three weathering facies are recognized but in the nearby well, 16/3-6, a deeper truncation have taken place and only the altered coherent rock facies is preserved below Upper Jurassic sandstones (Fig. 9C).

The application of outcrop studies has been demonstrated to increase the understanding of how reservoir properties were formed and destroyed in deeply buried paleoregolith profiles during subaerial exposure. The results will help when reconstructing erosional patterns and predicting areas with better reservoir potential in subsurface paleoregoliths, but caution must be applied to the impact of physical and chemical compaction on reservoir quality during burial.

Acknowledgements

This study has been funded by Lundin Norway AS. Access to the cores presented in this study has kindly been granted by Lundin Norway AS. XRD and SEM analyses at the University of Oslo were carried out under the kind supervision of Maarten Aerts and Berit Løken Berg. Support

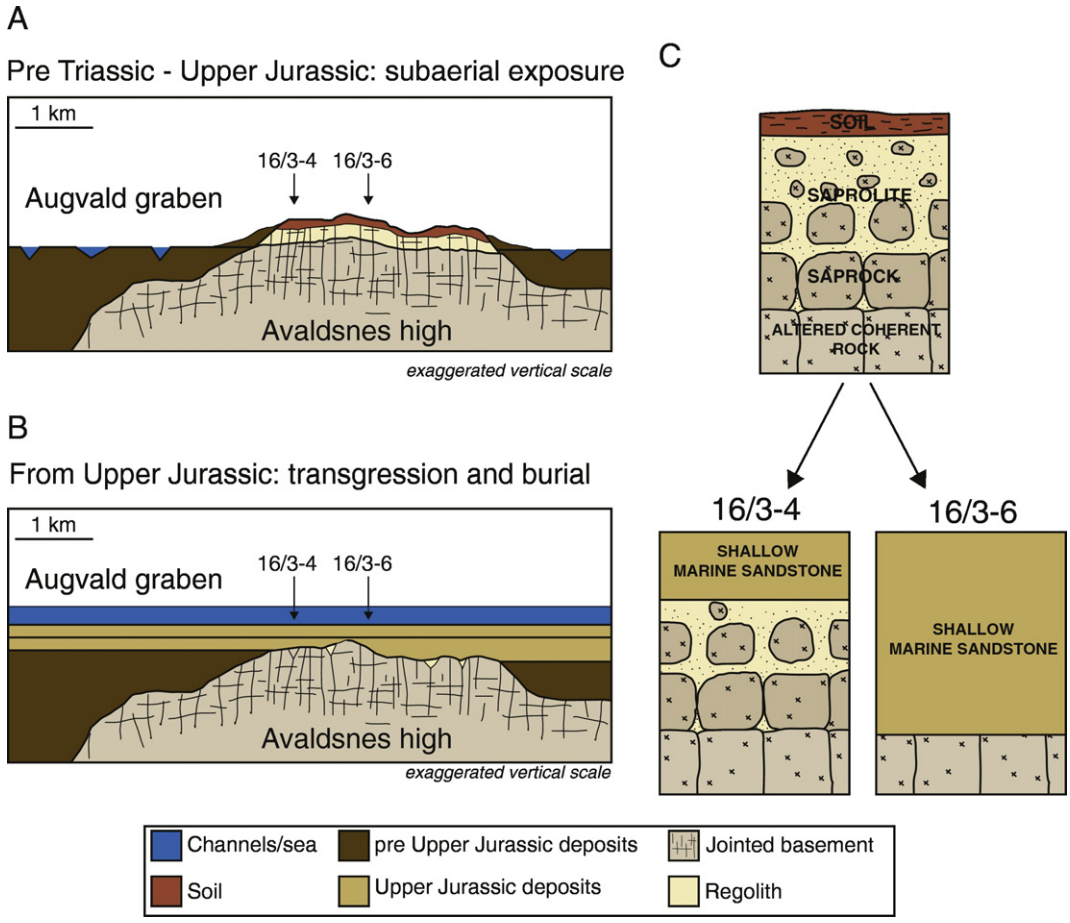

Fig. 9. Conceptual model showing: A) Development of regolith mantle on the Avaldsnes high from pre Triassic to late Jurassic. B) Erosion, transgression and burial of the Avaldsnes high from late Jurassic until present. C) Differences in depth of truncation may explain the variation in preservation of weathering facies in 16/3-4 and 16/3-6.

to PAS came from the NSF-CZO program. Thanks to Bobby Harrison for allowing access to the Keystone Blue quarry and to Jeff Sanders for your hospitality when we visited the Sparta quarry. Thanks to Adrian Read for improving the language of the paper. We are grateful for valuable improvements to earlier versions of this paper proposed by Gary Stinchcomb and three anonymous reviewers.

References

Abbink, O., Targarona, J., Brinkhuis, H., Visscher, H., 2001. Late Jurassic to earliest Cretaceous palaeoclimatic evolution of the southern North Sea. Glob. Planet. Chang. 30, 231–256.

Acworth, R.I., 1987. The development of crystalline basement aquifers in a tropical environment. Q. J. Eng. Geol. Hydrogeol. 20, 265–272.

Ahlberg, A., Olsson, I., Šimkevičius, P., 2003. Triassic–Jurassic weathering and clay mineral dispersal in basement areas and sedimentary basins of southern Sweden. Sediment. Geol. 161:15–29. http://dx.doi.org/10.1016/S0037-0738(02)00381-0.

Asbjørnsen, E., 2015. Sedimentology, Petrology and Diagenesis of Core 16/1-13 from the Edvard Grieg Field, Utsira High, Norwegian North Sea. University of Oslo (Unpublished master thesis). (95 pp).

Bahlburg, H., Dobrzinski, N., 2011. Chapter 6: A review of the Chemical Index of Alteration (CIA) and its application to the study of Neoproterozoic glacial deposits and climate transitions. In: Arnaud, E., Halverson, G.P., Shields-Zhou, G. (Eds.), The Geological Record of Neoproterozoic Glaciations. Geological Society, London, Memoirs 36: pp. 81–92. http://dx.doi.org/10.1144/M36.6.

Battiau-Queney, Y., 1996. A tentative classification of paleoweathering formations based on geomorphological criteria. Geomorphology 16, 87–102.

Bazilevskaya, E., Lebedeva, M., Pavich, M., Rother, G., Parkinson, D.Y., Cole, D., Brantley, S.L., 2013. Where fast weathering creates thin regolith and slow weathering creates thick regolith. Earth Surf. Process. Landf. 38, 847–858.

Bazilevskaya, E., Rother, G., Mildner, D.F., Pavich, M., Cole, D., Bhatt, M.P., Jin, L., Steefel, C.I., Brantley, S.L., 2015. How oxidation and dissolution in diabase and granite control porosity during weathering. Soil Sci. Soc. Am. J. 79, 55–73.

Bergbauer, S., Martel, S.J., 1999. Formation of joints in cooling plutons. J. Struct. Geol. 21, 821–835.

Berner, E.K., Berner, R.A., 2012. Global Environment: Water, Air, and Geochemical Cycles. Princeton University Press (488 pp).

Borrelli, L., Perri, F., Critelli, S., Gullà, G., 2012. Minero-petrographical features of weathering profiles in Calabria, southern Italy. Catena 92, 196–207.

Brantley, S., White, T., White, A., Sparks, D., Richter, D., Pregitzer, K., Derry, L., Chorover, J., Chadwick, O., April, R., 2006. Frontiers in Exploration of the Critical Zone: Report of a Workshop Sponsored by the National Science Foundation (NSF), October 24–26, 2005. Newark, DE (30 pp).

Brantley, S.L., Goldhaber, M.B., Ragnarsdottir, K.V., 2007. Crossing disciplines and scales to understand the Critical Zone. Elements 3:307–314. http://dx.doi.org/10.2113/gselements.3.5.307.

Buss, H.L., Sak, P.B., Webb, S.M., Brantley, S.L., 2008. Weathering of the Rio Blanco quartz diorite, Luquillo Mountains, Puerto Rico: coupling oxidation, dissolution, and fracturing. Geochim. Cosmochim. Acta 72:4488–4507. http://dx.doi.org/10.1016/j.gca.2008.06.020.

Claeys, P.F., Mount, J.F., 1991. Diagenetic origin of carbonate, sulfide and oxide inclusions in biotites of the Great Valley Group (Cretaceous), Sacramento Valley. California. J. Sediment. Res. 61.

Cuong, T., Warren, J.K., 2009. Bach Ho field, a fractured granitic rservoir, Cuu Long Basin, offshore SE Veitnam: a "Buried-Hill" play. J. Pet. Geol. 32, 129–155.

Curtis, C., Spears, D., 1971. Diagenetic development of kaolinite. Clay Clay Miner. 19, 219–227.

Dewandel, B., Lachassagne, P., Wyns, R., Maréchal, J., Krishnamurthy, N., 2006. A generalized 3-D geological and hydrogeological conceptual model of granite aquifers controlled by single or multiphase weathering. J. Hydrol. 330:260–284. http://dx.doi.org/10.1016/j.jhydrol.2006.03.026.

Driese, S.G., McKay, L.D., Penfield, C.P., 2001. Lithologic and pedogenic influences on porosity distribution and groundwater flow in fractured sedimentary saprolite: a new application of environmental sedimentology. J. Sediment. Res. 71, 843–857.

Driese, S.G., Medaris Jr., L.G., Ren, M., Runkel, A.C., Langford, R.P., 2007. Differentiating pedogenesis from diagenesis in early terrestrial paleoweathering surfaces formed on granitic composition parent materials. J. Geol. 115, 387–406.

Eggleton, R.A., Taylor, G., Le Gleuher, M., Foster, L.D., Tilley, D.B., Morgan, C.M., 2008. Regolith profile, mineralogy and geochemistry of the Weipa Bauxite, northern Australia. Aust. J. Earth Sci. 55, S17–S43.

Fletcher, R., Buss, H., Brantley, S., 2006. A spheroidal weathering model coupling porewater chemistry to soil thicknesses during steady-state denudation. Earth Planet Sci. Lett. 244, 444–457.

Fredin, O., Zwingmann, H., Knies, J., Sorlie, R., Grandal, E.M., Lie, J.E., Müller, A., Vogt, C., 2014. Saprolites on- and offshore Norway: new constraints on formation processes and age. Program with Abstracts, 31st Nordic Geological Winter Meeting, 8–10 January, Lund, Sweden, p. 132.
Gilg, H.A., Hall, A.M., Ebert, K., Fallick, A.E., 2013. Cool kaolins in Finland. Palaeogeogr. Palaeoclimatol. Palaeoecol. 392:454–462. http://dx.doi.org/10.1016/j.palaeo.2013.09.030.
Goldich, S.S., 1938. A study in rock-weathering. J. Geol. 46, 17–58.
Graham, R.C., Rossi, A.M., Hubbert, K.R., 2010. Rock to regolith conversion: producing hospitable substrates for terrestrial ecosystems. GSA Today 20:4–9. http://dx.doi.org/10.1130/GSAT57A.1.
Grammer, G.M., Harris, P.M.M., Eberli, G.P., 2004. Integration of outcrop and modern analogs in reservoir modeling: overview with examples from the Bahamas. Integration of Outcrop and Modern Analogs in Reservoir Modeling. AAPG Memoir 80, pp. 1–22.
Gregersen, U., Michelsen, O., Sørensen, J.C., 1997. Stratigraphy and facies distribution of the Utsira Formation and the Pliocene sequences in the northern North Sea. Mar. Pet. Geol. 14, 893–914.
Hallam, A., Crame, J.A., Mancenido, M.O., Francis, J., Parrish, J.T., 1993. Jurassic climates as inferred from the sedimentary and fossil record (and discussion). Philos. Trans. R. Soc. Lond. Ser. B Biol. Sci. 341, 287–296.
Hillier, S., 2000. Accurate quantitative analysis of clay and other minerals in sandstones by XRD: comparison of a Rietveld and a reference intensity ratio (RIR) method and the importance of sample preparation. Clay Miner. 35, 291–302.
Huang, W.H., 1974. Stabilities of kaolinite and halloysite in relation to weathering of feldspars and nepheline in aqueous solution. Am. Mineral. 59, 365–371.
International Society for Rock Mechanics Commission on Standardization of Laboratory and Field Tests (ISRM), 1978n. Suggested methods for the quantitative description of discontinuities in rock masses. Int. J. Rock. Mech. Min. Sci. 15, 319–368.
Jin, L., Rother, G., Cole David, R., Mildner David, F.R., Duff Christopher, J., Brantley Susan, L., 2011. Characterization of deep weathering and nanoporosity development in shale—a neutron study. Am. Mineral. (498 pp).
Joussein, E., Petit, S., Churchman, J., Theng, B., Righi, D., Delvaux, B., 2005. Halloysite clay minerals—a review. Clay Miner. 40, 383–426.
Kogure, T., Murakami, T., 1996. Direct identification of biotite/vermiculite layers in hydrobiotite using high-resolution TEM. Mineral. J. 18, 131–137.
Krauskopf, K.B., Bird, D.K., 1995. Introduction to Geochemistry 721. McGraw-Hill, New York (647 pp).
Ksienzyk, A.K., Jacobs, J., Fossen, H., Dunkl, I., Košler, J., 2013. The basement of the Utsira High: U/Pb, (U/Th)/He and fission track thermochronology. Abstracts and Proceedings of the Geological Society of Norway. Norwegian Geological Winter Meeting 2013. Oslo, January 8–10, p. 75.
Ksienzyk, A.K., Jacobs, J., Fossen, H., Woznitza, T., Wemmer, K., Dunkl, I., 2016. Comparing offshore and onshore thermal histories: low-T thermochronology of the Utsira High, western Norway. EGU General Assembly Conference 2016, Vienna, 17–22 April. 18, p. 11723.
Lervik, K.-S., 2006. Triassic lithostratigraphy of the Northern North Sea Basin. Nor. J. Geol. 86, 93–116.
Le Pera, E., Sorriso-Valvo, M., 2000. Weathering and morphogenesis in a Mediterranean climate, Calabria, Italy. Geomorphology 34, 251–270.
Liboriussen, J., Ashton, P., Tygesen, T., 1987. The tectonic evolution of the Fennoscandian Border Zone in Denmark. Tectonophysics 137:21–29. http://dx.doi.org/10.1016/0040-1951(87)90310-6.
Lidmar-Bergström, K., 1982. Pre-Quaternary geomorphological evolution in southern Fennoscandia. Geological Survey of Sweden, C 785 (202 pp).
Lidmar-Bergström, K., 1993. Denudation surfaces and tectonics in the southernmost part of the Baltic Shield. Precambrian Res. 64:337–345. http://dx.doi.org/10.1016/0301-9268(93)90086-H.
Lidmar-Bergström, K., 1995. Relief and saprolites through time on the Baltic Shield. Geomorphology 12:45–61. http://dx.doi.org/10.1016/0169-555X(94)00076-4.
Lidmar-Bergström, K., 1999. Uplift histories revealed by landforms of the Scandinavian domes. Geol. Soc. Lond., Spec. Publ. 162:85–91. http://dx.doi.org/10.1144/GSL.SP.1999.162.01.07.
Lidmar-Bergström, K., Olsson, S., Olvmo, M., 1997. Palaeosurfaces and associated saprolites in southern Sweden. Geol. Soc. Lond., Spec. Publ. 120:95–124. http://dx.doi.org/10.1144/GSL.SP.1997.120.01.07.
Lin, H., 2010. Earth's Critical Zone and hydropedology: concepts, characteristics, and advances. Hydrol. Earth Syst. Sci. 14, 25–45.
Liivamägi, S., Somelar, P., Vircava, I., Mahaney, W.C., Kirs, J., Kirsimäe, K., 2015. Petrology, mineralogy and geochemical climofunctions of the Neoproterozoic Baltic paleosol. Precambrian Res. 256:170–188. http://dx.doi.org/10.1016/j.precamres.2014.11.008.
Lundegårdh, H., 1978. The Vånga Granite in southernmost Sweden. Geological Survey of Sweden (23 pp).
Lundmark, A., Sæther, T., Sørlie, R., 2013. Ordovician to Silurian magmatism on the Utsira High, North Sea: implications for correlations between the onshore and offshore Caledonides. Geol. Soc. Lond. Spec. Publ. 390, 513–523.
Markewich, H., Pavich, M., Buell, G., 1990. Contrasting soils and landscapes of the Piedmont and Coastal Plain, eastern United States. Geomorphology 3:417–447. http://dx.doi.org/10.1016/0169-555X(90)90015-I.
McKie, T., Williams, B., 2009. Triassic palaeogeography and fluvial dispersal across the northwest European Basins. Geol. J. 44:711–741. http://dx.doi.org/10.1002/gj.1201.
Meunier, A., 2005. Clays. Springer-Verlag, Berlin Heidelberg, Berlin.
Migoń, P., 1997. Palaeoenvironmental significance of grus weathering profiles: a review with special reference to northern and central Europe. Proc. Geol. Assoc. 108:57–70. http://dx.doi.org/10.1016/S0016-7878(97)80006-5.
Molina, E., García González, M.T., Espejo, R., 1991. Study of paleoweathering on the Spanish hercynian basement Montes de Toledo (Central Spain). Catena 18, 345–354.
Moore, D.M., Reynolds, R.C., 1997. X-ray Diffraction and the Identification and Analysis of Clay Minerals. Oxford University Press, Oxford (xviii, 378 pp).
Nahon, D.B., 1991. Self-organization in chemical lateritic weathering. Geoderma 51, 5–13.
Navarre-Sitchler, A., Brantley, S.L., Rother, G., 2015. How porosity increases during incipient weathering of crystalline silicate rocks. Rev. Mineral. Geochem. 80, 331–354.
Naqvi, S.A.A.-E., 2013. Weathering of Precambrian Basement and Formation of Sedimentary Particles in Scania. Unpublished master thesis. University of Oslo (108 pp).
Négrel, P., 2006. Water–granite interaction: clues from strontium, neodymium and rare earth elements in soil and waters. Appl. Geochem. 21:1432–1454. http://dx.doi.org/10.1016/j.apgeochem.2006.04.007.
Nelson, R.A., 2001. Geological Analysis of Naturally Fractured Reservoirs. Gulf Professional Publication, Boston (332 pp).
Nelson, R., Moldovanyi, E., Matcek, C., Azpiritxaga, I., Bueno, E., 2000. Production characteristics of the fractured reservoirs of the La Paz field, Maracaibo basin, Venezuela. AAPG Bull. 84, 1791–1809.
Nesbitt, H.W., Young, G.M., 1989. Formation and diagenesis of weathering profiles. J. Geol. 97, 129–147.
Nesbitt, H.W., Fedo, C.M., Young, G.M., 1997. Quartz and feldspar stability, steady and non-steady-state weathering, and petrogenesis of siliciclastic sands and muds. J. Geol. 105, 173–192.
Nystuen, J.P., Kjemperud, A.V., Müller, R., Adestàl, V., Schomacker, E., 2014. Late Triassic–Early Jurassic climatic change, northern North Sea region: impact on alluvial architecture, paleosols and clay mineralogy. From Depositional Systems to Sedimentary Successions on the Norwegian Continental Margin. IAS Special Publications 46, pp. 59–100.
Nøttvedt, A., Johannessen, E.P., Surlyk, F., 2008. The mesozoic of western Scandinavia and East Greenland. Episodes 31, 59–65.
Oberhardt, N., 2013. Granite Weathering, Saprolitization and the Formation of Secondary Clay Particles, SW Bornholm. Unpublished master thesis. University of Oslo (109 pp).
O'Brien, E., Buol, S., 1984. Physical transformations in a vertical soil-saprolite sequence. Soil Sci. Soc. Am. J. 48, 354–357.
Olesen, O., Dehls, J.F., Ebbing, J., Henriksen, H., Kihle, O., Lundin, E., 2006. Aeromagnetic mapping of deep-weathered fracture zones in the Oslo Region — a new tool for improved planning of tunnels. Nor. J. Geol. 87, 253–267.
Olesen, O., Pascal Kierulf, H., Brönner, M., Dalsegg, E., Fredin, O., Solbakk, T., 2013. Deep weathering, neotectonics and strandflat formation in Nordland, northern Norway. Nor. J. Geol. 93, 189–213.
Pacheco, F.A., Van der Weijden, C.H., 2012. Weathering of plagioclase across variable flow and solute transport regimes. J. Hydrol. 420, 46–58.
Pagliai, M., Kutilek, M., 2008. Soil micromorphology and soil hydraulics. New Trends in Soil Micromorphology. Springer, pp. 5–18.
Papoulis, D., Tsolis-Katagas, P., Katagas, C., 2004. Progressive stages in the formation of kaolin minerals of different morphologies in the weathering of plagioclase. Clay Clay Miner. 52:275–286. http://dx.doi.org/10.1346/CCMN.2004.0520303.
Parizek, J.R., Girty, G.H., 2014. Assessing volumetric strains and mass balance relationships resulting from biotite-controlled weathering: implications for the isovolumetric weathering of the Boulder Creek Granodiorite, Boulder County, Colorado, USA. Catena 120, 29–45.
Rainbird, R., Nesbitt, H., Donaldson, J., 1990. Formation and diagenesis of a sub-Huronian saprolith: comparison with a modern weathering profile. J. Geol. 801–822.
Ramm, M., 1992. Porosity-depth trends in reservoir sandstones: theoretical models related to Jurassic sandstones offshore Norway. Mar. Pet. Geol. 9, 553–567.
Rebertus, R., Weed, S., Buol, S., 1986. Transformations of biotite to kaolinite during saprolite-soil weathering. Soil Sci. Soc. Am. J. 50, 810–819.
Reynolds III, R.C., Reynolds Jr., R.C., 2012. NEWMOD II a Computer Program for the Calculation of One-dimensional Diffraction Patterns of Mixed-layered Clays 1526 Farlow Avenue, Crofton, MD 21114, USA.
Retallack, G., 2001. Soils of the Past: An Introduction to Paleopedology. second ed. Blackwell Science, London.
Riber, L., Dypvik, H., Sørlie, R., 2015. Altered basement rocks on the Utsira High and its surroundings, Norwegian North Sea. Nor. J. Geol. 93, 57–89.
Riber, L., Dypvik, H., Sørlie, R., Ferrell Jr., R.E., 2016. Clay minerals in deeply buried paleoregoliths, Norwegian North Sea. Clays Clay Miner. http://dx.doi.org/10.1346/CCMN.2016.064036.
Richter, D.D., Yaalon, D.H., 2012. "The changing model of soil" revisited. Soil Sci. Soc. Am. J. 76, 766–778.
Rietveld, H.M., 1969. A profile refinement method for nuclear and magnetic structures. J. Appl. Crystallogr. 2, 65–71.
Roaldset, E., Pettersen, E., Longva, O., Mangerud, J., 1982. Remnants of preglacial weathering in western Norway. Nor. J. Geol. 62, 169–178.
Roaldset, E., Riis, F., Johnsen, S.O., 1993. Weathered basement rocks below Mesozoic sediments, Norwegian North Sea. In: Ford, D., McCann, B., Vajocczki, S. (Eds.), Programme with Abstracts, Third International Geomorphology Conference, 23–28 August. Hamilton, Ontario, Canada, p. 229.
Scarciglia, F., Le Pera, E., Critelli, S., 2007. The onset of the sedimentary cycle in a mid-latitude upland environment: weathering, pedogenesis, and geomorphic processes on plutonic rocks (Sila Massif, Calabria). Geol. Soc. Am. Spec. Pap. 420, 149–166.
Schoeneberger, P., Amoozegar, A., 1990. Directional saturated hydraulic conductivity and macropore morphology of a soil-saprolite sequence. Geoderma 46, 31–49.
Schroeder, P.A., Kim, J.G., Melear, N.D., 1997. Mineralogical and textural criteria for recognizing remnant Cenozoic deposits on the Piedmont: evidence from Sparta and Greene County, Georgia, U.S.A. Sediment. Geol. 108:195–206. http://dx.doi.org/10.1016/S0037-0738(96)00054-1.

Schroeder, P.A., West, L.T., 2005. Weathering profiles developed on granitic, mafic, and ultramafic terrains in the area of Elberton, Georgia. Georgia Geological Society Guidebook 25, pp. 55–80.
Selvikvåg, B., 2012. Sedimentology and Facies Analysis of the Late Triassic Luno Conglomerate Member of the Skagerrak Formation, Southern Viking Graben, North Sea. University of Bergen (Unpublished master thesis), (140 pp).
Sheldon, N.D., Tabor, N.J., 2009. Quantitative paleoenvironmental and paleoclimatic reconstruction using paleosols. Earth Sci. Rev. 95:1–52. http://dx.doi.org/10.1016/j.earscirev.2009.03.004.
Slagstad, T., Davidsen, B., Daly, J.S., 2011. Age and composition of crystalline basement rocks on the Norwegian continental margin: offshore extension and continuity of the Caledonian-Appalachian orogenic belt. J. Geol. Soc. Lond. 168, 1167–1185.
Srivastava, P., Sauer, D., 2014. Thin-section analysis of lithified paleosols from Dagshai Formation of the Himalayan Foreland: identification of paleopedogenic features and diagenetic overprinting and implications for paleoenvironmental reconstruction. Catena 112, 86–98.
Stangvik, K., 2015. Weathering Trends and Secondary Clay-Mineral Formation in Monzogranites from Georgia, USA. Unpublished master thesis. University of Oslo (86 pp).
Steel, R., Ryseth, A., 1990. The Triassic–Early Jurassic succession in the northern North Sea: megasequence stratigraphy and intra-Triassic tectonics. Geol. Soc. Lond., Spec. Publ. 55, 139–168.
Stober, I., Bucher, K., 2007. Hydraulic properties of the crystalline basement. Hydrogeol. J. 15:213–224. http://dx.doi.org/10.1007/s10040-006-0094-4.
Stormer Jr., J.C., Whitney, J.A., Hess, J.R., 1980. Petrology and geochemistry of the Elberton Granite. In: Stormer Jr., J.C., Whitney, J.A. (Eds.), Geological, Geochemical, and Geophysical Studies of the Elberton Batholith, Eastern Georgia 1910–30. Department of Natural Resources Guidebook, Atlanta, Georgia.
Storvoll, V., Bjørlykke, K., Mondol, N.H., 2005. Velocity-depth trends in Mesozoic and Cenozoic sediments from the Norwegian Shelf. AAPG Bull. 89, 359–381.
Surlyk, F., Sørensen, A.M., 2010. An early Campanian rocky shore at Ivö Klack, southern Sweden. Cretac. Res. 31:567–576. http://dx.doi.org/10.1016/j.cretres.2010.07.006.
Sutton, S., Maynard, J.B., 1992. Multiple alteration events in the history of a sub-Huronian regolith at Lauzon Bay, Ontario. Can. J. Earth Sci. 29, 432–445.
Sutton, S., Maynard, J.B., 1993. Sediment-and basalt-hosted regoliths in the Huronian supergroup: role of parent lithology in middle Precambrian weathering profiles. Can. J. Earth Sci. 30, 60–76.
Sutton, S., Maynard, J.B., 1996. Basement unconformity control on alteration, St. Francois Mountains, SE Missouri. J. Geol. 55–70.
Sørlie, R., Maast, T.E., Amundsen, H.E.F., Hammer, E., Charnock, M., Throndsen, I., Riber, L., Mearns, E.W., Dorn, A., Cummings, J., Fredin, O., 2014. Petrographic and samarium-neodymium isotope signatures of the Johan Sverdrup discovery, Norwegian North Sea. Paper Presented at The "Brae Play" South Viking Graben, Aberdeen.
Sørlie, R., Riber, L., Dypvik, H., 2016. Altered basement rocks as sediment source and reservoir — the southern Utsira High, Norwegian North Sea. Program with Abstracts, 32nd Nordic Geological Winter Meeting, 13–15 January, Helsinki, Finland.
Tan, P., Oberhardt, N., Dypvik, H., Riber, L., Ferrell Jr., R.E., 2017. Weathering profiles and clay mineralogical developments, Bornholm, Denmark. Mar. Pet. Geol. 80, 32–48.
Taylor, J.C., 1991. Computer programs for standardless quantitative analysis of minerals using the full powder diffraction profile. Powder Diffract. 6, 2–9.
Thiry, M., Schmitt, J.M., Simon-Coinçon, R., 1999. Problems, progress and future research concerning palaeoweathering and palaeosurfaces. In: Thiry, M., Simon-Coinçon (Eds.), Palaeoweathering, Palaeosurfaces and Related Continental Deposits. Special Publications of the IAS 27, pp. 1–17.
Tsuzuki, Y., Kawabe, I., 1983. Polymorphic transformations of kaolin minerals in aqueous solutions. Geochim. Cosmochim. Acta 47:59–66. http://dx.doi.org/10.1016/0016-7037(83)90090-X.
Vail, P., Mitchum Jr., R., Thompson III, S., 1977. Seismic stratigraphy and global changes of sea level: part 4. Global cycles of relative changes of sea level: section 2. Application of seismic reflection configuration to stratigraphic interpretation. In: Payton, C.E. (Ed.), Seismic Stratigraphy — Applications to Hydrocarbon Exploration. American Association of Petroleum Geologists Special Publication Vol. M26, pp. 83–97.
Vajda, V., Wigforss-Lange, J., 2009. Onshore Jurassic of Scandinavia and related areas. GFF 131:5–23. http://dx.doi.org/10.1080/11035890902975309.
Velde, B.B., Meunier, A., 2008. The Origin of Clay Minerals in Soils and Weathered Rocks. Springer Science & Business Media (406 pp).
Weaver, C.E., 1989. Clays, muds, and shales. Developments in Sedimentology 44. Elsevier, Amsterdam (819 pp).
Webb, H.N., Girty, G.H., 2016. Residual regolith derived from the biotite-controlled weathering of Cretaceous tonalite–quartz diorite, Peninsular Ranges, southern California, USA: a case study. Catena 137, 459–482.
White, A.F., Brantley, S.L., 2003. The effect of time on the weathering of silicate minerals: why do weathering rates differ in the laboratory and field? Chem. Geol. 202:479–506. http://dx.doi.org/10.1016/j.chemgeo.2003.03.001.
Whitney, D.L., Evans, B.W., 2010. Abbreviations for names of rock-forming minerals. Am. Mineral. 95, 185.
Wright, V.P., 1986. Pyrite formation and the drowning of a palaeosol. Geol. J. 21, 139–149.
Wright, E.P., Burgess, W., 1992. The hydrogeology of crystalline basement aquifers in Africa. Geol. Soc. Spec. Publ. 66, 1–27.
Zauyah, S., Schaefer, C.E.G.R., Simas, F.N.B., 2010. Saprolites. In: Stoops, G. (Ed.), Interpretation of Micromorphological Features in Soils and Regoliths. Elsevier Science, pp. 49–68.
Ziegler, P.A., 1992. North Sea rift system. Tectonophysics 208:55–75. http://dx.doi.org/10.1016/0040-1951(92)90336-5.
Ziegler, K., Longstaffe, F.J., 2000. Multiple episodes of clay alteration at the Precambrian/Paleozoic unconformity, Appalachian basin: isotopic evidence for long-distance and local fluid migrations. Clay. Clay Miner. 48, 474–493.
Åberg, G., Kornfält, K.-A., Nord, A.G., 1985. The Vånga granite, south Sweden—a complex granitic intrusion. GFF 107:153–159. http://dx.doi.org/10.1080/11035898509452628.